

Wavelength conversion using semiconductor optical amplifiers in differential Mach-Zehnder interferometer with tunable input coupler

A. Bhardwaj, J.E. Simsarian, J.D. LeGrange, L. Zhang, P. Bernasconi, N. Sauer, L. Buhl and D.T. Neilson

A monolithically-integrated wavelength converter on an InP platform with a semiconductor optical amplifier in each arm of a differential Mach-Zehnder interferometer is presented. The data input has a tunable coupler that adjusts the splitting ratio of the optical power sent to each arm. Wavelength conversion at 40 Gbit/s is demonstrated and a conversion penalty of <2 dB is found when less optical power is sent to the delayed arm.

Introduction: Wavelength converters based on semiconductor optical amplifiers, when combined with passive wavelength-routing devices, have the potential to replace electronic routing functions in communications networks [1, 2]. The key performance requirements for wavelength converters used for data routing are low bit error ratio (BER) penalties and fast gain and phase recovery times, particularly for high data rates such as 40 and 100 Gbit/s. Monolithic integration of wavelength converters with an integrated tunable source reduces the number of fibre couplings, thereby simplifying the packaging requirements [3, 4].

Previously, we reported on a monolithically-integrated differential wavelength converter with equal interferometer arm lengths for the probe path, but unequal arm lengths for the data-modulated pump to create short output pulses [5]. The data pump power was split equally between the two Mach-Zehnder arms and the BER penalty for wavelength conversion was 5 dB.

We demonstrate in this Letter a new design for a monolithically-integrated wavelength converter on an indium phosphide (InP) platform with a semiconductor optical amplifier (SOA) in each arm of a Mach-Zehnder interferometer (MZI). The key feature differentiating this device from those previously reported is a tunable coupler in the data path, which controls the splitting ratio of the data signal to the SOAs in the two arms, as shown in Fig. 1. This allows us to adjust the bit delayed by ΔT at SOA2 to have a lower peak power than an undelayed bit at SOA1, which results in a better matching of the delayed and undelayed pulse temporal profiles. Therefore, pulse reshaping of the wavelength-converted signal is accomplished without the need to bias the SOAs in the MZI asymmetrically. The symmetrically-biased SOAs exhibit similar gain and nonlinear response, resulting in better extinction and lower distortion of the wavelength-converted output. In this Letter, we describe the fabrication and operation of the wavelength converter with a tunable input coupler and present results on its performance.

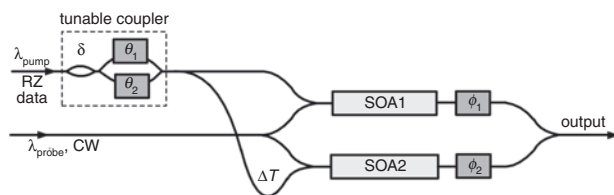


Fig. 1 Schematic diagram of wavelength converter

Device design and fabrication: Every split or combination junction of the device shown in Fig. 1 is a Y-branch with approximately 0.5 splitting ratio. The differential delay between the pump inputs to the MZI with the SOAs is designed to be 8.33 ps, one-third of a bit period at 40 Gbit/s. The arms of this MZI have thermo-optic phase shifters that tune, ϕ_1 and ϕ_2 , which adjust the relative phase between the two arms.

The tunable coupler [6] is designed using two coupled MZIs, one with a fixed relative phase delay, δ (designed to be 120°), between its two arms and the other with thermo-optic phase shifters that tune θ_1 and θ_2 to adjust the relative phase between its two arms and control the optical-power coupling ratio. The coupling ratio of this design is less sensitive to variations in wavelength and fabrication in comparison to a single-stage splitter. We measured the coupling ratio over the wavelength range 1535–1557 nm, and found it to deviate by <0.03 from the average for coupling ratios between 0.5 and 0.7. The coupling ratio is

defined as $\beta_{pump} = P_{SOA1}/(P_{SOA1} + P_{SOA2})$, where P_{SOA1} and P_{SOA2} are the optical powers at SOA1 and SOA2, respectively.

The fabrication of the wavelength converter uses an approach [7] that allows monolithic integration of low-loss passive optical waveguides with an active SOA. While the propagation loss of ~ 1 dB/cm is an important parameter of the passive guides, the carrier recovery time in the SOAs is often a limiting factor in the gain and phase dynamics of these nonlinear elements. To decrease the response time of the electrical carriers, we design the SOAs to have a high optical confinement in the active material and sufficient length to result in high saturation. The active/passive integration platform relies on buried rib-loaded passive waveguides and buried-heterostructure active regions, where the active SOA sections are grown with butt-joints to the passive guides.

The wafers are grown via low-pressure MOCVD and consist of ~ 400 nm passive guiding layers ($\lambda_g \sim 1.3 \mu\text{m}$), which are selectively removed by etching in the areas reserved for the active regions. The bandgap for the bulk active material is $\lambda_g \sim 1.6 \mu\text{m}$ and a p -doped InP cap layer is grown over the entire wafer to ensure adequate growth uniformity and then selectively removed from the passive areas by etching. The passive waveguides are defined by a ~ 100 nm-thick rib obtained with a shallow etch, while the channel guide buried-heterostructure SOAs are generated through a deep etch. This is followed by the overgrowth of a current blocking layer, an isolation step, a second overgrowth of p -doped InP, and two metallisation steps, which form contacts to the SOAs and heaters for tuning the coupler and the phase shifters in the MZI. The active waveguide of the SOA is 1 mm long and $\sim 1 \mu\text{m}$ wide. The minimum bend radius of the passive waveguide is $620 \mu\text{m}$. The access waveguide at the facet is angled by 7° to suppress reflections but no antireflection coating was applied at the time of characterisation.

The packaged device is shown in Fig. 2. The 7.15×3.5 mm InP chip is indium soldered to a copper stud and electrical current is supplied through connections to a printed circuit board. Lensed fibres are attached to the InP chip, as can be seen in Fig. 2(a–c).

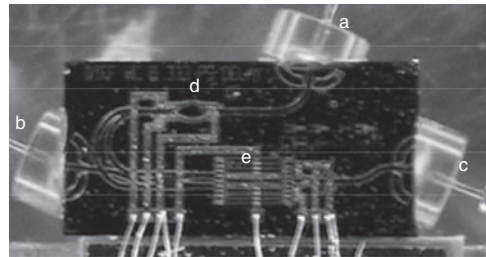


Fig. 2 Photograph of packaged monolithic wavelength converter device with parts identified

a data-pump input fibre; b CW-probe input fibre; c output fibre; d tunable coupler; e MZI and SOAs

Experiment and results: We used the experimental setup shown in Fig. 3 for wavelength conversion experiments. A pseudorandom bit sequence (PRBS) of length $2^{31} - 1$ modulates the light from a tunable laser (pump wavelength, $\lambda_{pump} = 1558.17$ nm) at 40 Gbit/s using a dual-drive LiNbO₃ Mach-Zehnder modulator. An electro-absorption modulator (EAM) acts as a pulse carver to generate RZ data pulses. Unmodulated light from a tunable laser ($\lambda_{probe} = 1547$ nm) is amplified using an erbium-doped fibre amplifier (EDFA) and injected simultaneously with the data pump into the wavelength converter. The input power to the wavelength converter for both the continuous-wave (CW) probe and data pump is $\sim +16.5$ dBm, giving approximately $+2$ dBm CW power at the SOA. Both SOAs are biased at 450 mA. At the output of the wavelength converter, a 0.6 nm-wide bandpass filter shapes the signal, which we previously found to be the optimal bandwidth. The filter is detuned by approximately 0.5 nm to the short-wavelength side of the probe wavelength, which enhances the blue-detuned sideband and reduces the inter-symbol interference. A 1 nm-wide bandpass filter further rejects amplified spontaneous emission noise from the SOAs and the pump signal. We detect the signal with a preamplified receiver with a 1 nm-wide bandpass filter between two EDFAs. The output of the photodiode goes to a 40 Gbit/s error detector that measures the BER of the wavelength-converted light. The BER curves against optical signal-to-noise ratio (OSNR) referenced to 0.1 nm resolution bandwidth are shown in Fig. 4 along with a

wavelength-converted eye diagram. The optical power at the input to the preamplified receiver is -31.9 dBm for the back-to-back measurement at $\text{BER} = 1 \times 10^{-9}$.

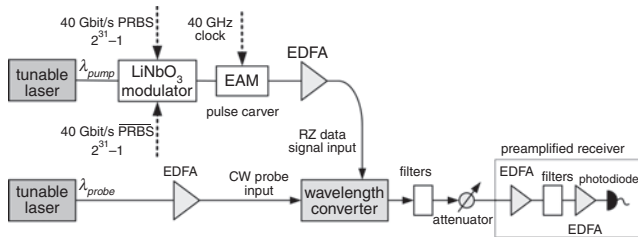


Fig. 3 Experimental setup to characterise wavelength conversion

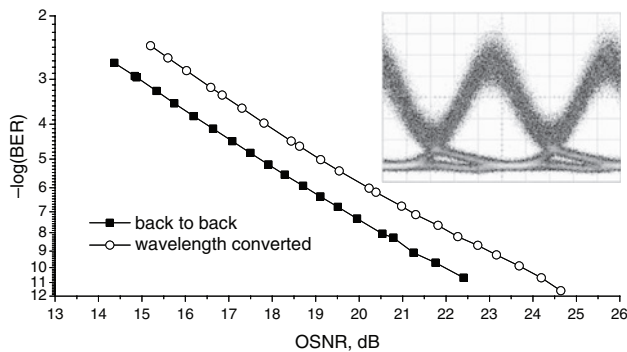


Fig. 4 BER against OSNR (referenced to 0.1 nm resolution bandwidth) and eye diagram for wavelength conversion between $\lambda_{\text{pump}} = 1558.17$ nm and $\lambda_{\text{probe}} = 1547$ nm

The optical power coupling ratio of the input data and phase of the MZI were adjusted to minimise the wavelength conversion penalty. The lowest penalty for wavelength conversion was found to be 1.8 dB. The coupling ratio at this condition corresponds to a 2 to 1 power ratio at the SOAs with the greater power at SOA1.

Conclusions: We have demonstrated a monolithically-integrated wavelength converter with SOAs in each arm of a differential Mach-Zehnder interferometer. The device has a tunable coupler on the pump input, which allows the amount of light sent to each arm to be varied. We found a low wavelength conversion penalty when less pump power is sent to the SOA with a longer signal path to it, resulting in dynamic balancing of the nonlinear response of the SOAs in the MZI. The device achieves an OSNR penalty of <2 dB with no error floor observed.

Acknowledgment: This work was carried out under contract FA8750-04-C-0013 as part of DARPA MTO's DOD-N programme.

© The Institution of Engineering and Technology 2009
23 December 2008

Electronics Letters online no: 20093696
doi: 10.1049/el:20093696

A. Bhardwaj, J.E. Simsarian, L. Zhang, P. Bernasconi, N. Sauer, L. Buhl and D.T. Neilson (Bell Laboratories, Alcatel-Lucent, 791 Holmdel-Keypoint Road, Holmdel, NJ 07733, USA)

E-mail: ashishb@ece.ucsb.edu

J.D. LeGrange (LGS Innovations, 15 Vreeland Road, Florham Park, NJ 07932-1506, USA)

A. Bhardwaj: Now with the Department of Electrical and Computer Engineering, University of California, Santa Barbara, CA 93106, USA

References

- Gripp, J., Simsarian, J.E., Bernasconi, P., LeGrange, J.D., Zhang, L., Buhl, L., Stiliadis, D., Neilson, D.T., and Zirngibl, M.: 'Load-balanced optical packet router based on 40 Gbit/s wavelength converters and time buffers'. Proc. European Conf. on Optical Communications, ECOC, 2005, Vol. 6, pp. 51–52
- Stubkjaer, K.E.: 'Semiconductor optical amplifier-based all-optical gates for high-speed optical processing', *IEEE J. Sel. Top. Quantum. Electron.*, 2000, 6, (6), pp. 1428–1435
- Bernasconi, P., Zhang, L., Yang, W., Sauer, N., Buhl, L.L., Sinsky, J.H., Kang, I., Chandrasekhar, S., and Neilson, D.T.: 'Monolithically integrated 40-Gbit/s switchable wavelength converter', *J. Lightwave Technol.*, 2006, 24, (1), pp. 71–76
- Lal, V., Mašanović, M.L., Summers, J.A., Fish, G., and Blumenthal, D.J.: 'Monolithic wavelength converters for high-speed packet-switched optical networks', *IEEE J. Sel. Top. Quantum. Electron.*, 2007, 13, (1), pp. 49–57
- Bernasconi, P., Zhang, L., Yang, W., Buhl, L., Sauer, N., Bhardwaj, A., Gripp, J., Simsarian, J.E., and Neilson, D.T.: 'Monolithically integrated differential Mach-Zehnder filter for 40 Gbit/s wavelength conversion in high-confinement butt-joint SOAs'. Indium Phosphide and Related Materials Conf., (IPRM), 2006, paper WA2.2
- Bhardwaj, A., Sauer, N., Buhl, L., Yang, W., Zhang, L., and Neilson, D.T.: 'An InP-based optical equalizer monolithically integrated with a semiconductor optical amplifier', *IEEE Photonics Technol. Lett.*, 2007, 19, (19), pp. 1514–1516
- Joyner, C.H., Doerr, C.R., Stulz, L.W., Centanni, J.C., and Zirngibl, M.: 'Low-threshold nine-channel waveguide grating router-based continuous wave transmitter', *J. Lightwave Technol.*, 1999, 17, (4), pp. 647–651